

Higher-order moments of the Mott-Smith shock approximation

Stefano Boccelli^{1,2}

¹NASA Goddard Space Flight Center

²NPP NASA Postdoctoral Fellow, Oak Ridge Associated Universities

email: `stefano.boccelli@nasa.gov`

2024

Abstract

This technical note reports the expression of selected higher-order moments associated with the Mott-Smith solution of the shock-wave profile. The considered moments are the pressure tensor, the heat-flux vector and tensor, the fourth-order double-tensor, its full contraction, and the fifth-order moment vector. The resulting shock profiles are shown for Mach 2 and Mach 10 conditions.

1 Introduction

The internal structure of a shock wave cannot be accurately described by the continuum theory. Instead, one should employ the kinetic theory of gases [1] that describes the evolution of the velocity distribution function (VDF) in phase space. The Mott-Smith method allows for a simple closed-form solution of this problem [2]. Despite its approximated nature and despite the present availability of accurate Monte-Carlo simulation tools, this method remains of interest due to its simplicity and widespread adoption [3, 4, 5, 6].

The original work by Mott-Smith describes the shock-wave structure in terms of density, velocity and temperature profiles. Later works [7, 4] also report the expression of the heat-flux vector and tensor. In this technical note, the analysis is extended to higher-order moments of the Mott-Smith VDF. These moments are meaningful non-equilibrium indicators, and are of interest to the development of moment methods [8, 9, 10].

1.1 The Mott-Smith approximation

This section briefly recaps the Mott-Smith approximation [2]. The velocity distribution function (VDF) is assumed to be composed of two Maxwellians,

$$f = f_\alpha + f_\beta. \quad (1)$$

Unless specified otherwise, in this work Greek subscripts identify the populations that compose the VDF while Roman subscripts denote the spacial components of a vector or a tensor.

The bulk velocity and temperature of the first population, u_α and T_α , are set to the free-stream values, while u_β and T_β refer to the post-shock gas state, and are found from the Rankine-Hugoniot jump relations. The additional constraint necessary to close the system is obtained by considering either second or third-order moments of the collision operator. Ultimately, the densities of the two populations are found to follow the relation

$$\begin{cases} \rho_\alpha/\rho_{\text{FS}} = 1/(1 + e^{Bx/\lambda_{\text{FS}}}), \\ \rho_\beta/\rho_{\text{FS}} = (u_\alpha/u_\beta)/(1 + e^{-Bx/\lambda_{\text{FS}}}), \end{cases} \quad (2)$$

where the physical position, x , is scaled with the free-stream mean-free-path, λ_{FS} . At $x = 0$, one has $\rho_\alpha = \rho_{\text{FS}}/2$. The parameter B , appearing in Eq. (2), is a function of the Mach number and its values are tabulated in the original work for selected molecular interaction potentials. The choice of the potential and of the moment employed to close the system are known to have an impact on the solution [11, 12]. However, this does not affect the derivations shown in this work. Notice that the results of this work also do not depend on the specific expression of the mean free path, but only on the dimensionless quantity x/λ_{FS} , that is here taken to be a single variable.

Considering an ideal gas, the pressure of the two populations is $P_\alpha = \rho_\alpha(k_{\text{B}}/m)T_\alpha$, where k_{B} and m are the Boltzmann constant and the molecular mass of the considered gas, and the same applies to β . The gas density, bulk velocity and pressure along the shock profile are¹

$$\begin{cases} \rho = \rho_\alpha + \rho_\beta, \\ u = (\rho_\alpha u_\alpha + \rho_\beta u_\beta)/\rho, \\ T = (\rho_\alpha T_\alpha + \rho_\beta T_\beta)/\rho + \frac{m}{3k_{\text{B}}}(\rho_\alpha \rho_\beta/\rho^2)(u_\alpha - u_\beta)^2, \end{cases} \quad (3)$$

and the pressure is $P = \rho(k_{\text{B}}/m)T$.

¹The original publication includes a typo in the temperature equation: $\rho_\alpha T_\alpha$ and $\rho_\beta T_\beta$ are subtracted, but should be added instead.

1.2 Moments of the distribution function

The statistical moments of a VDF, f , are defined as [1]

$$U_\psi = \iiint_{-\infty}^{+\infty} \psi f \, d^3v \equiv \langle \psi \rangle, \quad (4)$$

where ψ is a particle quantity. Choosing the particle mass, momentum or energy, $\psi = \{m, mv_i, mv^2/2\}$, results in the mass, momentum and energy densities of the whole gas,

$$\rho = \langle m \rangle, \quad \rho u_i = \langle mv_i \rangle, \quad \rho \varepsilon = \frac{1}{2} \langle mv^2 \rangle, \quad (5)$$

whose expressions, in the Mott-Smith approximation, are obtained from Eq. (3). In this work, we are also interested in the pressure tensor, P_{ij} , and in the heat-flux vector, q_i ,

$$P_{ij} = \langle mc_i c_j \rangle, \quad q_i = \frac{1}{2} \langle mc_i c_j c_j \rangle, \quad (6)$$

where $c_i = v_i - u_i$ is the peculiar velocity and where repeated indices imply summation. The hydrostatic pressure, P , is obtained from the trace of the pressure tensor: $P = P_{ii}/3$. Also, we are interested in the following moments: the full heat-flux tensor, Q_{ijk} , the partially-contracted fourth-order moment tensor, R_{ijkk} ,

$$Q_{ijk} = \langle mc_i c_j c_k \rangle, \quad R_{ijkk} = \langle mc_i c_j c_k c_k \rangle, \quad (7)$$

and the contracted fifth-order moment, S_{ijjkk} ,

$$S_{ijjkk} = \langle mc_i c_j c_j c_k c_k \rangle. \quad (8)$$

The fully-contracted fourth-order moment, R_{iiij} , is proportional to the kurtosis of the distribution function. To fix the ideas, a super-Maxwellian kurtosis is often associated with heavier-than-Maxwellian tails. At equilibrium, for a Maxwellian distribution, one has $Q_{ijk}^{\text{eq}} = S_{ijjkk}^{\text{eq}} = 0$, while the fourth-order moments are $R_{ijkk}^{\text{eq}} = 5P^2 \delta_{ij}/\rho$ (where δ_{ij} is the Kronecker delta), and $R_{iiij}^{\text{eq}} = 15P^2/\rho$. In this technical note, the analysis is limited to the mentioned moments, as they represent the first extension to the Euler and Navier-Stokes theories, and are commonly employed in third- and fourth-order moment methods [13, 14, 15, 16].

2 Moments of the Mott-Smith approximation

The first three moments of the Mott-Smith approximation, ρ , u and P , are obtained from Eq. (2). The computation of other moments is particularly simple, as the integrals of Eq. (4) apply separately to the two Maxwellians, f_α and f_β . The full pressure tensor is obtained as

$$P_{ij} = \langle mc_i c_j \rangle_\alpha + \langle mc_i c_j \rangle_\beta. \quad (9)$$

Considering the first integral, $\langle \dots \rangle_\alpha$, the calculation is simplified by rewriting the peculiar velocity as

$$c_i \equiv v_i - u_i = c_{i,\alpha} + \mathcal{U}_{i,\alpha}, \quad (10)$$

where $\mathcal{U}_{i,\alpha} = u_{i,\alpha} - u_i$ expresses the deviation of the average velocity of f_α from the bulk velocity of the whole distribution, f . Notice that $\mathcal{U}_{i,\alpha}$ has only one non-zero component, $\mathcal{U}_{i,\alpha} = \mathcal{U}_\alpha \delta_{ix} = (u_\alpha - u) \delta_{ix}$. This quantity is known along the shock profile from the Mott-Smith solution. Also, the quantity $c_{i,\alpha}$ is the peculiar velocity with respect to the bulk velocity of the α species, $c_{i,\alpha} = v - u_{i,\alpha}$, and can be used to easily compute the central moments associated with the α population. With these definitions,

$$\begin{aligned} \langle m c_i c_j \rangle_\alpha &= m \langle (c_{i,\alpha} + \mathcal{U}_{i,\alpha})(c_{j,\alpha} + \mathcal{U}_{j,\alpha}) \rangle_\alpha \\ &= m \langle c_{i,\alpha} c_{j,\alpha} + \mathcal{U}_{i,\alpha} c_{j,\alpha} + c_{i,\alpha} \mathcal{U}_{j,\alpha} + \mathcal{U}_{i,\alpha} \mathcal{U}_{j,\alpha} \rangle_\alpha \\ &= P_{ij,\alpha} + \rho_\alpha \mathcal{U}_{i,\alpha} \mathcal{U}_{j,\alpha}, \quad (11) \end{aligned}$$

where the terms involving odd-order powers of $c_{i,\alpha}$ are zero, since f_α is symmetric. Furthermore, one considers that the pressure tensor, $P_{ij,\alpha}$, is isotropic. Repeating the computation for f_β and adding the two contributions, one has

$$P_{ij} = (P_\alpha + P_\beta) \delta_{ij} + (\rho_\alpha \mathcal{U}_\alpha^2 + \rho_\beta \mathcal{U}_\beta^2) \delta_{ix} \delta_{jx}, \quad (12)$$

or,

$$\begin{cases} P_{xx} = P_\alpha + P_\beta + \rho_\alpha (u_\alpha - u)^2 + \rho_\beta (u_\beta - u)^2, \\ P_{yy} = P_{zz} = P_\alpha + P_\beta, \end{cases} \quad (13)$$

the remaining components being zero. As expected, this result shows anisotropy, as $P_{xx} \geq P_{yy} = P_{zz}$. In the free-stream and in the post-shock regions isotropy is recovered as either one of the two densities, or the respective velocity deviation, goes to zero.

The Mott-Smith heat-flux vector, $q_i = Q_{ijj}/2$, and the component Q_{xxx} of the heat-flux tensor, are discussed in [7]. Here, we report the expression of the full Q_{ijk} . The derivation is analogous to that of the pressure tensor (Eq. (11)), and gives

$$Q_{ijk} = (\mathcal{U}_\alpha P_\alpha + \mathcal{U}_\beta P_\beta) (\delta_{ij} \delta_{kx} + \delta_{ik} \delta_{jx} + \delta_{jk} \delta_{ix}) + (\rho_\alpha \mathcal{U}_\alpha^3 + \rho_\beta \mathcal{U}_\beta^3) \delta_{ix} \delta_{jx} \delta_{kx}. \quad (14)$$

The heat-flux vector is found by contracting Q_{ijk} . As expected from symmetry considerations, its only non-zero component is q_x , which reads

$$q_x = \frac{Q_{xjj}}{2} = \frac{1}{2} [\rho_\alpha \mathcal{U}_\alpha^3 + \rho_\beta \mathcal{U}_\beta^3 + 5\mathcal{U}_\alpha P_\alpha + 5\mathcal{U}_\beta P_\beta]. \quad (15)$$

With analogous computations, the fourth-order moment, R_{ijkk} , is found to be

$$\begin{aligned} R_{ijkk} &= [5P_\alpha^2/\rho_\alpha + \mathcal{U}_\alpha^2 P_\alpha + 5P_\beta^2/\rho_\beta + \mathcal{U}_\beta^2 P_\beta] \delta_{ij} \\ &\quad + [\rho_\alpha \mathcal{U}_\alpha^4 + 7\mathcal{U}_\alpha^2 P_\alpha + \rho_\beta \mathcal{U}_\beta^4 + 7\mathcal{U}_\beta^2 P_\beta] \delta_{ix} \delta_{jx}, \quad (16) \end{aligned}$$

that is composed of an isotropic part, augmented by an additional contribution in the (x, x) direction. Its contraction, the scalar quantity R_{ijjj} , is

$$R_{ijjj} = \rho_\alpha \mathcal{U}_\alpha^4 + 10 \mathcal{U}_\alpha^2 P_\alpha + 15 P_\alpha^2 / \rho_\alpha + \rho_\beta \mathcal{U}_\beta^4 + 10 \mathcal{U}_\beta^2 P_\beta + 15 P_\beta^2 / \rho_\beta. \quad (17)$$

Similarly, one can find the contracted fifth-order moment vector, whose only non-zero component is

$$S_{xjjkk} = \rho_\alpha \mathcal{U}_\alpha^5 + 14 \mathcal{U}_\alpha^3 P_\alpha + 35 \mathcal{U}_\alpha P_\alpha^2 / \rho_\alpha + \rho_\beta \mathcal{U}_\beta^5 + 14 \mathcal{U}_\beta^3 P_\beta + 35 \mathcal{U}_\beta P_\beta^2 / \rho_\beta. \quad (18)$$

Extension to N populations

Extensions of the Mott-Smith theory to a higher number of Maxwellian populations have been proposed in the past. For instance, Salwen et al [17] considered a distribution in the form $f = \sum_{\gamma=1}^N f_\gamma$, with $N = 3$ distinct populations. The expressions for the moments, discussed in this work, are easily extended to these cases by simply adding the contributions of the individual populations. For instance, the pressure tensor would read

$$P_{ij} = \sum_{\gamma=1}^N [P_\gamma \delta_{ij} + \rho_\gamma (u_\gamma - u)^2 \delta_{ix} \delta_{jx}], \quad (19)$$

and the other moments are obtained similarly.

3 Numerical computations

This section shows the shock structure for two Mach numbers, $M = 2$ and $M = 10$. These conditions are chosen arbitrarily, and are intended to span a large range of velocities. Above $M = 10$, the density profile becomes substantially insensitive to the free-stream velocity, as the parameter B changes only marginally [2].

First, the Mott-Smith solution is computed in terms of density, velocity and pressure, as detailed above. Figure 1-Left and -Center show the pressure and density profiles, rescaled with the free-stream and post-shock values. In these calculations, the parameter B was set to the value B_1 tabulated in the original work. The expressions of the higher-order moments remain valid for other choices of B .

Figure 1-Left also shows the pressure tensor components, P_{xx} and P_{yy} , obtained from Eq. (13), while the Center and Right boxes show the dimensionless moments, R_{ijjj}^* , Q_{xjj}^* and S_{xjjkk}^* , from Eqs. (17), (15) and (18), respectively. The non-dimensionalization (superscript “*”) is performed dividing the moments by the local density, ρ , and by suitable powers of the thermal velocity, $\sqrt{P/\rho}$,

$$\begin{cases} Q_{xjj}^* = Q_{xjj} / [\rho (P/\rho)^{3/2}] , \\ R_{ijjj}^* = R_{ijjj} / [\rho (P/\rho)^{4/2}] , \\ S_{xjjkk}^* = S_{xjjkk} / [\rho (P/\rho)^{5/2}] . \end{cases} \quad (20)$$

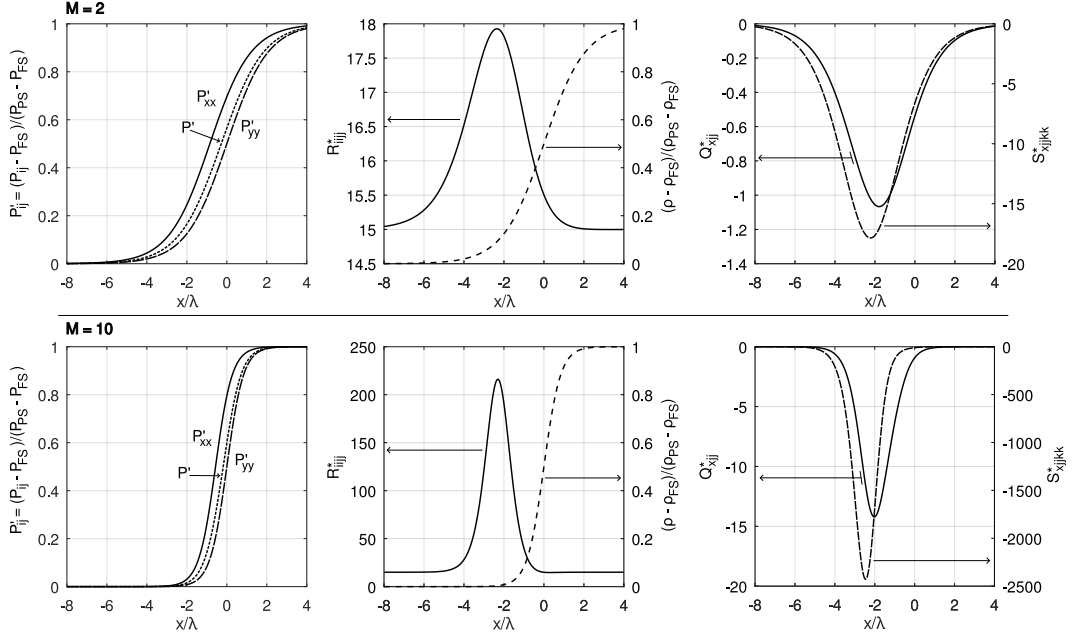


Figure 1: Shock wave profiles from the Mott-Smith model (with $B = B_1$, see [2]) for $M = 2$ (Top) and $M = 10$ (Bottom).

At equilibrium, $R_{ijij}^{\star \text{eq}} = 15$ and $Q_{xjj}^{\star \text{eq}} = S_{xjjkk}^{\star \text{eq}} = 0$. As one might expect, these moments depart significantly from equilibrium in the $M = 2$ shock, and reach extreme values in the $M = 10$ case.

The maximum of these moments is located upstream of the shock. This behavior of the higher-order moments is compatible with the previous observation by Muckenfuss [11] that the center of the temperature profile is located ahead of the center of the velocity profile, which in turn is ahead of the center of the density profile (located at $x = 0$). Although not shown directly in the figure, the heat-flux is located upstream of the temperature profile, and moments of higher order are generally further upstream. Notice that this phenomenon is well-known [13, 18], and is due to the increased sensitivity of higher-order moments to supra-thermal particles.

Data availability statement

This manuscript has no associated data.

Acknowledgements

This research was partially supported by an NPP (NASA Postdoctoral Program) appointment, administered by Oak Ridge Associated Universities (ORAU).

References

- [1] J. H. Ferziger and H. G. Kaper, *Mathematical theory of transport processes in gases*. London: North-Holland Publishing, 1972.
- [2] H. M. Mott-Smith, “The solution of the Boltzmann equation for a shock wave,” *Physical Review*, vol. 82, no. 6, p. 885, 1951.
- [3] M. A. Solovchuk and T. W. Sheu, “Prediction of shock structure using the bimodal distribution function,” *Physical Review E—Statistical, Nonlinear, and Soft Matter Physics*, vol. 81, no. 5, p. 056314, 2010.
- [4] M. Y. Timokhin, A. Kudryavtsev, and Y. A. Bondar, “The Mott-Smith solution to the regular shock reflection problem,” *Journal of Fluid Mechanics*, vol. 950, p. A14, 2022.
- [5] A. Bret and A. Pe’er, “On the width of a collisionless shock and the index of the cosmic rays it accelerates,” *The Astrophysical Journal*, vol. 968, no. 2, p. 100, 2024.
- [6] E. Yilmaz, G. Oblapenko, and M. Torrilhon, “On nonlinear closures for moment equations based on orthogonal polynomials,” *arXiv preprint arXiv:2407.05894*, 2024.
- [7] M. Nathenson and D. Baganoff, “Constitutive relations associated with the Mott-Smith distribution function,” *The Physics of Fluids*, vol. 16, no. 12, pp. 2110–2115, 1973.
- [8] I. Müller and T. Ruggeri, *Extended thermodynamics*. NY: Springer-Verlag New York, 1993.
- [9] M. Torrilhon, “Modeling nonequilibrium gas flow based on moment equations,” *Annual review of fluid mechanics*, vol. 48, pp. 429–458, 2016.
- [10] M. Timokhin and D. Rukhnikov, “Local non-equilibrium phase density reconstruction with Grad and Chapman-Enskog methods,” in *Journal of Physics: Conference Series*, vol. 1959, p. 012049, IOP Publishing, 2021.
- [11] C. Muckenfuss, “Some aspects of shock structure according to the bimodal model,” *The Physics of Fluids*, vol. 5, no. 11, pp. 1325–1336, 1962.

- [12] S. Ziering and F. Ek, “Mean-free-path definition in the Mott-Smith shock wave solution,” *The Physics of Fluids*, vol. 4, no. 6, pp. 765–766, 1961.
- [13] J. McDonald and M. Torrilhon, “Affordable robust moment closures for CFD based on the maximum-entropy hierarchy,” *Journal of Computational Physics*, vol. 251, pp. 500–523, 2013.
- [14] H. Struchtrup and M. Torrilhon, “Regularization of Grad’s 13 moment equations: Derivation and linear analysis,” *Physics of Fluids*, vol. 15, no. 9, pp. 2668–2680, 2003.
- [15] A. Alvarez Laguna, B. Esteves, A. Bourdon, and P. Chabert, “A regularized high-order moment model to capture non-Maxwellian electron energy distribution function effects in partially ionized plasmas,” *Physics of Plasmas*, vol. 29, no. 8, 2022.
- [16] S. Boccelli, P. Parodi, T. E. Magin, and J. G. McDonald, “Modeling high-Mach-number rarefied crossflows past a flat plate using the maximum-entropy moment method,” *Physics of Fluids*, vol. 35, no. 8, 2023.
- [17] H. Salwen, C. E. Grosch, and S. Ziering, “Extension of the Mott-Smith method for a one-dimensional shock wave,” *The Physics of Fluids*, vol. 7, no. 2, pp. 180–189, 1964.
- [18] J. Laplante and C. Groth, “Comparison of maximum entropy and quadrature-based moment closures for shock transitions prediction in one-dimensional gaseous theory,” in *AIP Conference Proceedings*, vol. 1786, AIP Publishing, 2016.